Influence of confinement in controlled-pore glass on the layer spacing of smectic-*A* liquid crystals

George Cordoyiannis,[1,2,*] Aleksander Zidanšek,[2] Gojmir Lahajnar,[2] Zdravko Kutnjak,[2] Heinz Amenitsch,[3] George Nounesis,[1] and Samo Kralj[2,4]

[1]*National Centre for Scientific Research "Demokritos," 153 10 Aghia Paraskevi, Greece*

[2]*Jožef Stefan Institute, P.O. Box 3000, 1001 Ljubljana, Slovenia*

[3]*Institute of Biophysics and Nanosystems Research, Austrian Academy of Sciences, Schmiedlstr. 6, A-8012 Graz, Austria*

[4]*Laboratory of Physics of Complex Systems, Faculty of Natural Sciences, University of Maribor, Koroška 160, 2000 Maribor, Slovenia*

(Received 17 December 2008; published 11 May 2009)

A detailed x-ray scattering study has been performed in the temperature range of the smectic-*A* phase for the liquid crystal compounds dodecylcyanobiphenyl (12CB) and octylcyanobiphenyl (8CB) confined in different controlled-pore glasses (CPGs) characterized by their average void radius R. On decreasing the temperature in bulk samples the layer thickness is increasing for 12CB and decreasing for 8CB, respectively. In nontreated CPG samples the layers dilate significantly with respect to the bulk liquid crystal. In order to explain the layer thickness behavior on varying temperature and R, one has to take into account molecular details of the liquid crystalline samples as well as memory effects.

DOI: 10.1103/PhysRevE.79.051703 PACS number(s): 61.30.Cz, 61.05.cf

I. INTRODUCTION

The randomly perturbed thermotropic liquid crystals (LCs) have attracted considerable interest so far [1,2]. One usually induces disorder to LCs either by mixing them with "impurities" or confining them to various porous matrices. Aerosil nanoparticles have been often used as impurities [2–6], which can form three qualitatively different random networks as the concentration of aerosils is varied [7–9]. Aerogels [10], Russian glasses [11], Vycor glasses [12], and controlled-pore glasses [13–15] are generally used as porous confining matrices. All these perturbation agents introduce into the system a new characteristic length scale R in addition to the disorder. In the case of aerosil nanoparticles this is the mean aerosil void size $R \sim 2/(a\rho_a)$, where ρ_a stands for the mass density of the aerosil particles and a is their active surface area [7]. In the case of porous matrices R stands for the average pore radius. Recent reports [2–4,6,14,16,17] reveal that the phase behavior of such perturbed LCs is dominantly influenced by R. The universal features observed are as follows. On decreasing R the temperature depression ΔT_c of phase-transition temperatures, with respect to bulk LC samples, typically increases. Below a critical value $R=R_c$, which is comparable to the relevant LC order-parameter correlation length ξ, a critical LC behavior is lost, i.e., the noncritical character of perturbers prevails. The main reasons behind such behavior are (i) disorder-induced spatially nonhomogeneous elastic frustrations, (ii) presence of a relatively large LC-perturbation agent interface, and (iii) finite-size effects.

All these phenomena arise from the interface interaction between the liquid crystal molecules and the disorder agents. Note that, in general, the interface invokes two competitive tendencies in such systems. If the interface is smooth on the size scale larger than ξ, then it locally acts as an ordering field. It suppresses the LC fluctuations, acting similarly as a reduced local effective temperature. On the larger scale randomness becomes apparent and hinders the ordering tendencies. An experimental manifestation of this competition was shown by Dadmun and Muthukumar [13] in their study of the isotropic (I) to nematic (N) phase behavior of *p*-azoxyanisole LC in controlled-pore glass (CPG) matrices. They observed increased T_c due to prevailing surface ordering effects for CPG samples characterized by $R \sim 150$ nm. However, in samples with $R \sim 20$ nm a decrease in T_c was observed, indicating a disorder-dominated regime. Additional studies have reported that with decreasing R the relative importance of disorder increases [14,16].

The competing surface ordering-disordering tendency can exhibit a complex behavior due to the presence of two qualitatively different fields describing LC ordering. The LC phases and structures are commonly reached via continuous symmetry-breaking phase transitions. The degree of ordering within a LC configuration is determined by an order-parameter field (OPF). On the other hand, the symmetry-breaking "direction" is described by symmetry-breaking field (SBF), also referred to as a gauge field [18]. These fields can respond to local perturbations on vastly different length scales. OPFs relax toward an equilibrium value on distances comparable to the order-parameter correlation length ξ, which reflects the intrinsic LC material properties if ξ is small with respect to the relevant confinement-imposed length R. Not so close to the critical temperature, the values of ξ are comparable to several nm. On the other hand, SBF is susceptible to R. For example, if a frustration is imposed on SBF at surfaces separated by a distance R, then the field exhibits gradual changes over all the available space in order to accommodate the imposed constraint. This is due to the existence of Goldstone fluctuation modes in SBFs, which can be excited relatively easy. Extreme susceptibility to perturbations is manifested also via the Imry-Ma theorem [19]. It claims that the quenched random disorder destroys the long-range order of SBF in the pure sample for arbitrary weak disorder. However, the validity of this concept is still disputable and it is not the subject of this article. Therefore, large-scale geometry strongly influences SBFs which can also in-

*george.cordoyiannis@fys.kuleuven.be

directly but essentially influence the OPFs via a SBF-OPF coupling. An example of a continuous symmetry-breaking of the orientational ordering is the isotropic to nematic (*I*-*N*) transition. In the *N* phase the ordering can be well described by the nematic director field $\vec{n}$ (SBF) and the uniaxial nematic orientational order parameter *S* (OPF). A simple example of a continuous translational symmetry breaking is represented by the nematic to smectic *A* (Sm*A*) transition. In the Sm*A* phase the ordering is typically described by the phase factor ϕ (SBF) and the translational order parameter η (OPF).

Most studies so far have focused on the phase behavior, i.e., on OPFs. Less attention has been paid to investigations concerning the structural properties [2,6,20]. Several such studies have analyzed the universal type behavior, e.g., validity of the Imry-Ma theorem for domain-type structural ordering. In smectic phases there is also interest about the behavior of the average smectic layer thickness as a function of *R*. In the case of LC-aerosil mixtures it was found that the layer spacing *d*, in different smectic phases and for various LCs, is reduced with respect to that of the bulk compound. Possible mechanisms behind this layer shrinkage have been worked out in detail in [6].

In order to contribute to the knowledge of this field, the small-angle x-ray scattering (SAXS) technique was employed to study the influence of CPG confinement on the smectic *A* phase layer spacing of LCs. The octylcyanobiphenyl (8CB) and the dodecylcyanobiphenyl (12CB) liquid crystals have been used, confined in treated and nontreated CPGs with a wide range of porous radii *R*. It is shown that even in the bulk 8CB and 12CB LC samples the temperature dependences $d(T)$ are qualitatively different. In most of CPG samples the smectic layers become dilated with respect to the bulk samples. The observations can be interpreted by taking into account the molecular details of the LCs and memory effects. This means that the behavior in this case is nonuniversal.

The plan of the paper is as follows. Section II is devoted to a description of the CPG samples and of the experimental setup. The results are presented in Sec. III and summarized in the last section. In the Appendix a simple Landau-Ginsburg–de Gennes type description of smectic ordering is presented, together with the main reason for a different phase behavior in the 8CB and 12CB samples.

II. SAMPLES AND EXPERIMENTAL SETUP

The liquid crystals 8CB and 12CB used in this study consist of the two phenyl rings and the octyl or dodecyl carbon tail, respectively. The prevailing belief is that the pure bulk 8CB undergoes a second-order Sm*A*-*N* phase transition on reducing the temperature *T*, with effective critical exponents between three-dimensional (3D) -*XY* and tricritical values [21]. This transition takes place at $T=T_{NA}\sim 307$ K. On the other hand, 12CB enters the Sm*A* phase directly from the isotropic (*I*) phase via a first-order phase transition at $T_{IA}\sim 332$ K [22].

Controlled-pore glass matrices were chosen as confining media. The CPG voids resemble curved and strongly interconnected cylinders of radii *R*. CPG matrices of the mean pore diameter ranging from 15.1 to 292 nm, with a standard deviation of 5–10 %, were used. The void surface of the CPGs is smooth down to the nm scale [23]. A scanning electron micrograph (SEM) of an empty CPG matrix with a porous diameter $R=72.9$ nm is shown in Fig. 1.

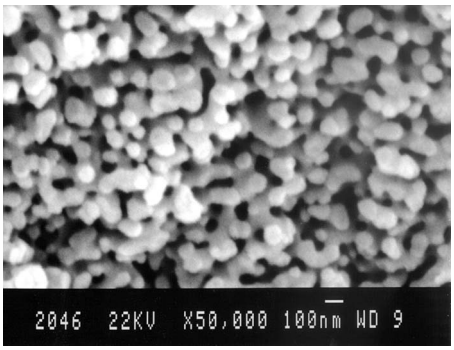

FIG. 1. A typical structure of a CPG matrix with a porous diameter of $R=72.9$ nm, measured by SEM.

The CPG void surfaces were either nontreated or treated with silane. The nontreated CPG void surfaces enforce the isotropic tangential orientational anchoring to LC molecules [13]. However, the orientation along the long axis of a void is preferred, on average, due to the steric effects. In silane-treated CPG samples the pore surface enforces a homeotropic orientational anchoring [14]. The CPG matrices were filled with LCs in temperatures deep in the isotropic phase of the latter.

The measurements of 12CB were performed in the Centre for Crystallography of Macromolecules (National Centre for Scientific Research "Demokritos," Athens, Greece). For measuring the smectic layer thickness *d* temperature dependence of 12CB, the samples were heated up to the *I* phase and then cooled down slowly to the Sm*A* phase. The measurements were performed at selected temperatures after the sample was slowly cooled and then stabilized for sufficient time. The samples were loaded into Hilgenberg Mark capillaries (tubes no. 14) and afterwards mounted on a heating stage (Instec Inc.) that achieves temperature stability of ± 10 mK. A Rigaku RUH3R rotating anode generator was used, operating at 5 kW and in the K_a line of Cu. The monochromator was consisted of a flat graphite and the beam was focused by double focusing mirrors (Molecular Structure Corporation). The detector was an *R*-Axis IV double imaging plate system 30×30 cm^2 (Molecular Structure Corporation). The resolution of this apparatus is 0.004 Å^{-1} (half width at half maximum).

The 8CB samples were measured at Austrian SAXS beamline of the ELETTRA Synchrotron (Trieste, Italy). The SAXS beamline uses a flat, asymmetric-cut double crystal monochromator and a double focusing toroidal mirror as optics to get a focused x-ray beam with an energy of 8 keV [24]. The samples were loaded in Hilgenberg Mark capillaries (tubes no. 14) and mounted on an in-house-built heating system. Its temperature was controlled by a water bath (Huber Unistat). This setup has a resolution better than 0.001 Å^{-1} (half width at half maximum).

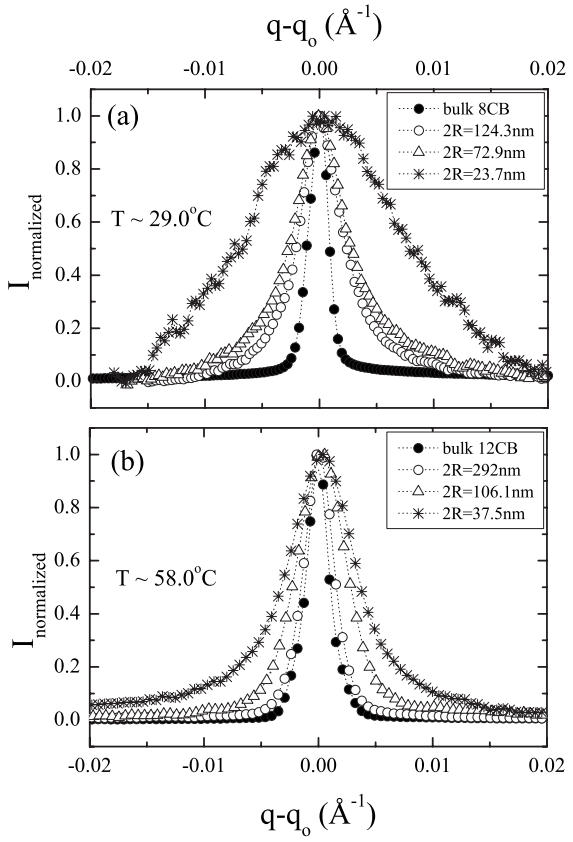

FIG. 2. The normalized-intensity profiles $I(q-q_o)$ of the quasi-Bragg smectic peaks in bulk and CPG-confined samples. Data (a) for 8CB samples are shown on the top layer and (b) for 12CB on the bottom layer, respectively.

We used two different thermal histories of the 8CB samples, to which we henceforth refer as *history 1* and *history 2*. In the history 1 case the sample was heated deep into the isotropic phase at 60 °C, remained there for 30 min, and then cooled down into the nematic phase at 40 °C and further into the smectic phase. Four or five temperature points were measured per 1 K in 3 min intervals between the vicinal points in the nematic and smectic phases. The exposure time was between 10 and 40 s depending on the strength of the signal. In the history 2 case the sample was heated into the isotropic phase at 50 °C and then cooled down into the nematic phase at 40 °C and further into the smectic phase. One or two temperature points were measured per 1 K in 3 min intervals. The exposure time was 10 s. The main differences between the two histories are the temperature of heating the sample in the *I* phase and the time remaining at it before the cooling process started.

III. RESULTS

In Fig. 2 the typical x-ray scattering intensity profiles $I(q)$ as a function of the scattering wave vector q for 8CB [Fig. 2(a)] and 12CB [Fig. 2(b)] bulk and confined samples are shown. With decreasing R the $I(q)$ spectrum progressively broadens for both LC compounds.

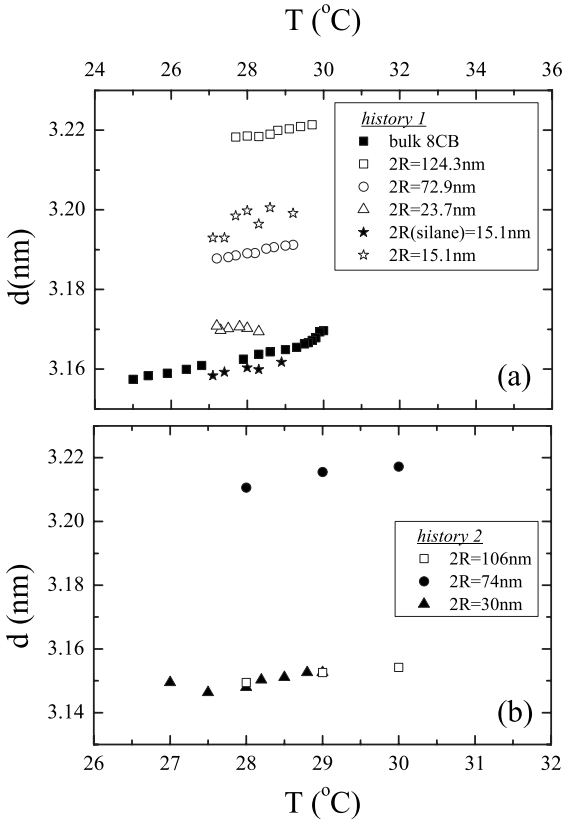

FIG. 3. The average smectic layer thickness d of 8CB as a function of temperature, in bulk and confined samples. Data corresponding (a) to history 1 are shown on the top layer and (b) the ones of history 2 on the bottom layer. The error in the determination of d is in the order of 0.0005 nm (not visible in the plot).

The behavior of smectic layer thickness d_b of bulk samples as a function of temperature is shown in Fig. 3 for 8CB and in Fig. 4 for 12CB, respectively. Comparing $d(T)$ results in Figs. 3 and 4 it is obvious that the bulk sample

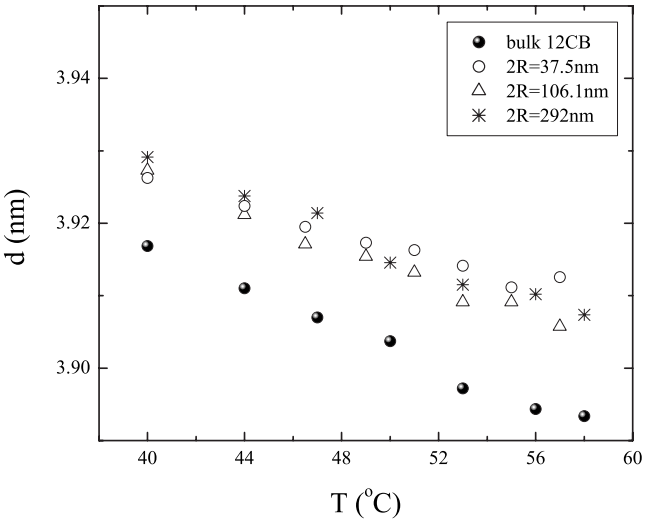

FIG. 4. The average smectic layer thickness d of 12CB as a function of temperature in bulk and CPG-confined samples. The error in the determination of d is in the order of 0.0015 nm.

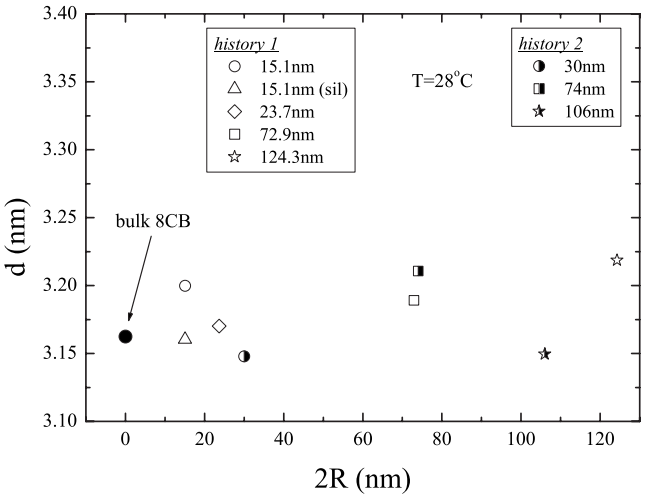

FIG. 5. The average smectic layer thickness d of all 8CB samples (history 1 and history 2) as a function of the CPG diameter $2R$. The error in the determination of d is in the order of 0.0005 nm.

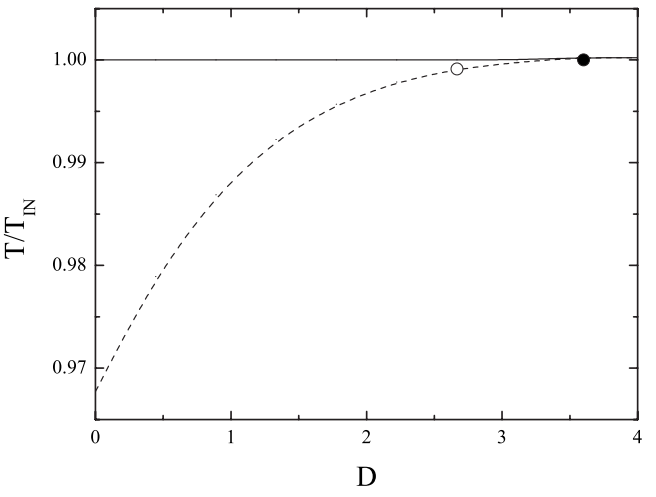

FIG. 6. The phase-transition behavior as a function of the coupling strength D, which is related to the length of flexible carbon tails. Open circle denotes the $D_c^{(1)}$ and the solid circle the $D_c^{(2)}$.

temperature behavior is qualitatively different in 8CB and 12CB, as already observed by Urban *et al.* [25]. In 8CB the layer thickness is slightly decreasing [Fig. 3(a)] on decreasing T. For example, $d_b(T\sim 30\ ^\circ\mathrm{C})\sim 3.17$ nm and $d_b(T\sim 26\ ^\circ\mathrm{C})\sim 3.16$ nm. In contrast, the layer thickness of 12CB (Fig. 4) is increasing on decreasing T. The temperature dependence is roughly linear, where $d_b(T\sim 58\ ^\circ\mathrm{C})\sim 3.89$ nm and $d_b(T\sim 40\ ^\circ\mathrm{C})\sim 3.92$ nm.

The influence of CPG confinement is as follows. In all CPG samples the trends of $d(T)$ variations are qualitatively similar with respect to the bulk LCs. Therefore, upon decreasing T the layer thickness is decreasing in 8CB samples and increasing in 12CB samples, respectively. In general, confinement gives rise to an apparent layer dilation with respect to the bulk behavior in all nontreated samples. In 8CB samples the layer thickness exhibits a rather complex behavior on varying R, which is for a given temperature ($T\sim 28\ ^\circ\mathrm{C}$) plotted in Fig. 5. Note that the observed variations in d are small (in the order of 0.02 nm). Furthermore, the values of d apparently depend on history of samples. Results for the histories 1 and 2 are plotted in Figs. 3(a) and 3(b), respectively. In contrast to 8CB samples, the layer thickness of 12CB samples, which was measured in a different experiment, exhibits relatively weak dependence on R for the set of CPG samples studied. The layer thickness $d(T)$ in the silanized sample with $2R=15.1$ nm is comparable to $d_b(T)$.

IV. DISCUSSION

Let us consider first the behavior of bulk samples. We claim that the layer thickness temperature dependence is influenced by LC molecular features. The continuum picture, which is presented in the Appendix, is not sufficient in this respect. Therefore, it only provides a rough insight into the behavior of the system. The bulk layer spacing $d_b=2\pi/q_0$ enters the elastic free-energy term [Eq. (A7)] as a phenomenological parameter. The nature of phase transition into the SmA phase, on lowering temperature, is dominantly influenced by the coupling strength [constant D in Eq. (A6)] between the translational and orientational LC order parameter [26]. This in turn depends on the length of LC carbon tails. The value of D for 8CB is close to its tricritical point $D_c^{(1)}$ (see Fig. 6). As a result, the N-SmA transition could be either continuous ($D_c^{(1)}<D$) or weakly discontinuous ($D_c^{(1)}>D$), depending on the sample purity that influences the value of D. In the case of 12CB the relation $D_c^{(1)}\gg D$ holds and the SmA phase is reached directly from the isotropic phase. Consequently, the fluctuations in the orientational order parameter are considerably stronger in the SmA phase of the 12CB. In the case of 8CB, the fluctuations are substantially reduced due to the existence of the intermediate N phase stability region [15].

A plausible explanation behind the observed $d_b(T)$ behavior, by decreasing temperature, in the bulk samples is as follows. For 8CB the layer thickness is dominantly influenced by the two relatively rigid phenyl rings. Thermal fluctuations of the rings are decreasing and consequently the rings in neighboring smectic layers are getting closer. On the other hand, in 12CB the flexible dodecyl carbon tails give rise to a different scenario. On entering the SmA phase the tails somewhat retain their "melted" state of the isotropic phase. At even lower temperatures the extent of their fluctuations calms down, resulting in a longer average tail length and in a larger d_b value. Therefore, the rigid part of LC molecules tends to decrease d_b, while the flexible part enforces the opposite behavior. The temperature behavior $d_b(T)$ depends on the balance between the competing tendencies. On increasing the flexible part (in our case the alkyl chain length n) of the molecule, a crossover in the behavior is expected that reflects in the change of sign of $\Delta d(T)=d_b(T<T_c)-d_b(T_c)$, where T_c stands for the transition temperature into a SmA phase. This is strongly supported by a recent study of Urban *et al.* [25] on n-cyanobiphenyls with various alkyl chain lengths ($n=8,9,10,11,12,14$) by means of x rays. They observed a change in the sign of Δd at $n=11$. They claimed that, by decreasing temperature, the number of kinks in the alkyl chain decreases resulting in the reduction

of the molecular length. The present conclusions are also in accordance with the measurements of Anesta *et al.* [27]. Their measurements show $\Delta d(T)<0$ for 8CB and $\Delta d(T)>0$ for $\bar{8}$S5 and $\overline{10}$S5. The latter two smectic LCs possess a flexible link between the core phenyl rings in contrast to 8CB. Therefore, in smectic LCs exhibiting relatively strong flexibility (e.g., longer alkyl chains) one expects $\Delta d(T)>0$.

Hereinafter, the confined samples are considered. In all nontreated samples one observes dilatation of the smectic layers with respect to the bulk samples. Possible mechanisms responsible for dilatations are (i) finite-size effects, (ii) randomness, and (iii) surface-induced memory effects. Finite-size effects are expected to increase the layer thickness. A pure confinement (i.e., without LC-CPG interaction) on average decreases the number of first neighbors of a LC molecule. Consequently, the average coupling strength with surrounding LC molecules is decreased and weaker interactions give rise to increased separation of smectic layers. Note that the specific-heat behavior [14], close to the *N*-Sm*A* phase transition, is dominated by finite-size effects in nontreated CPG samples. In order to estimate maximal number N_{LC} of packed LC molecules in radial direction we assume that LC molecules are oriented along the local long axis of a CPG void. Consequently $N_{\mathrm{LC}}\sim 2R/a$, where $a\sim 2$ nm estimates thickness of a LC molecule. In the sample with largest pore radius ($2R\sim 300$ nm) one gets $N_{\mathrm{LC}}\sim 150$. If finite-size effects would dominate the layer thickness behavior, then $d-d_b$ would decrease on increasing R, which is not observed here.

We further consider the influence of randomness. It is expected that a static disorder has a similar influence as the thermal disorder (i.e., thermal fluctuations). Therefore, according to our analysis described above, it should have different effects in 8CB and 12CB samples (i.e., layer dilatation in 8CB and layer compression in 12CB LCs), which is not observed in the present work. Furthermore, studies of the smectic layer thickness in LC and aerosil mixtures [6] suggest that the influence of disorder on d is relatively weak. In these systems a random-field type of disorder arises due to a random network formed by the aerosil nanoparticles. However, a shrinking of the smectic layers is observed in mixtures, revealing the dominance of other mechanisms [6].

We claim that a dominant mechanism behind layer dilatation is memory effect. The LC molecules in contact with a smooth (at a LC molecular scale) bounding surface can get frozen in [28] due to relatively strong LC-substrate local interactions. For example, such memorization could give rise to chevron structures even in the Sm*A* phase [29,30]. In our samples the memorized patterns are different for 8CB and 12CB LCs. In samples with 12CB the Sm*A* phase is entered from the *I* phase on decreasing temperature. In the Sm*A* phase the CPG surface reduces extent of molecular fluctuations. Consequently, the flexible chains get elongated and the imprinted smectic ordering on the surface has larger thickness in comparison to its bulk value. The resulting frozen-in periodicity slightly dilates the smectic layers within the CPG pores. In this scenario the layer dilatation does not depend on R for large enough values of R (with respect to the molecular scale). On the contrary, for 8CB the smectic ordering is entered from the nematic phase on lowering the temperature. In this case in the *N* phase nematiclike ordering is imprinted on a void's surface, which does not prefer any periodicity. On entering the Sm*A* phase the confined LC attains periodic structure. Conclusively, an elastic stress is established tending to make structure of frozen-in and "free" LC molecules comparable. This triggers a partial rearrangement of imprinted LC molecules (most probably via desorption and absorption mechanisms), resulting in periodic profile with slightly larger smectic layer thickness with respect to d_b. Thus, the established surface periodicity in this case also dilates the smectic layers of the sample. Note that the nematic history might be statistically different for different sample preparations, giving rise to history-dependent values of d, which is in line with our observations (see Fig. 3).

In the silanized 8CB sample, characterized by $2R=15.1$ nm, $d(T)$, and $d_b(T)$ dependencies are similar. In this sample homeotropic anchoring is established, promoting smectic growth from the surface toward interior. In this case different scenarios can result depending on the commensurability and incommensurability of d and R, as it was demonstrated in [31].

V. CONCLUSIONS

The small-angle x-ray scattering technique was used to study the temperature variations of the average smectic layer thickness d (in the Sm*A* phase) of bulk and in CPG-matrices-confined 8CB and 12CB samples with various pore diameters. It is found that the layer thickness behavior depends on the LC molecular features. In the bulk samples the $d(T)$ exhibits qualitatively different behavior for 8CB and 12CB LC, in line with other recent observations [25,27]. In 8CB the layer thickness is dominated by the rigid phenyl rings. On decreasing the temperature the extent of fluctuations of phenyl rings is decreasing, enabling a closer packing of the molecules. As a consequence, the value of d decreases, respectively. On the contrary, in 12CB the role of flexible dodecyl carbon tails is also significant. Upon decreasing the temperature, the fluctuations of the flexible tails are suppressed, their effective length is increasing thus resulting in an increase of d. In LCs confined to nontreated CPG cavities we observe layer dilation. The mechanisms behind this are the finite-size effects and the surface memory effects. Our results suggest that the latter is dominant. The surface memory effects are particularly pronounced for 8CB samples, where the smectic phase is entered from the nematic phase.

APPENDIX: SIMPLE THEORETICAL DESCRIPTION OF SMECTIC ORDERING

In this appendix a simple phenomenological description of the LC ordering is presented. Our focus is on the character of the transition into the Sm*A* phase and on the smectic structure. For this purpose the Landau–de Gennes–Ginzburg [26,32] type phenomenological description of LC ordering is used. The orientational ordering is described in terms of the nematic tensor order parameter Q. In the uniaxial approxi-

mation, where biaxial effects are neglected, the order parameter is conventionally expressed as [26,32]

$$Q = S(\vec{n} \otimes \vec{n} - I/3). \tag{A1}$$

Here $\vec{n}$ stands for the director field and S for the orientational uniaxial order parameter S. The unit vector field $\vec{n}$ points along the LC molecular local average uniaxial orientation and S describes the extent of fluctuations about $\vec{n}$. Therefore, $S=0$ in the isotropic phase. On the contrary, the relation $S=1$ signals perfectly aligned LC molecules. The Sm*A* layering is described in terms of the complex order parameter

$$\psi = \eta e^{i\phi}. \tag{A2}$$

The phase field ϕ locates the smectic layers. For the layers stacked along the wave vector $\vec{q}_0$ the phase is given by $\phi(\vec{r}) = \vec{q}_0 \cdot \vec{r}$. The translational order-parameter field η reveals the degree of translational ordering, i.e., the relation $\eta(\vec{r}) = 0$ signals absence of local translational ordering.

A thermotropic liquid crystal exhibiting either the *I*-*N*-Sm*A* or the *I*-Sm*A* phase transition is considered below. The free energy F of the confined LC is expressed as

$$F = \int (f_h^{(n)} + f_h^{(s)} + f_e + f_c) d^3r + \int (f_i^{(n)} + f_i^{(s)}) d^2r, \tag{A3}$$

where the volume integral runs over the LC body and the surface integral over the LC-CPG interface. In the simplest case of isotropic elasticity and in the lowest-order approximation (with respect to order-parameter expansions) the free-energy densities are expressed as

$$f_h^{(n)} = a_0^{(n)}(T - T_*) TrQ^2 - b^{(n)} TrQ^3 + c^{(n)}(TrQ^2)^2, \tag{A4}$$

$$f_h^{(s)} = a_0^{(s)}(T - T_{NA})|\psi|^2 + b^{(s)}|\psi|^4, \tag{A5}$$

$$f_c = -D\vec{\nabla}\psi \cdot Q\vec{\nabla}\psi^*, \tag{A6}$$

$$f_e = L|\vec{\nabla}Q|^2 + C(|\vec{n} \times \vec{\nabla}\psi|^2 + |(\vec{n} \cdot \vec{\nabla} - iq_0)\psi|^2), \tag{A7}$$

$$f_i^{(n)} = W_n \vec{\nu} \cdot Q \cdot \vec{\nu}, \tag{A8}$$

$$f_i^{(s)} = -\frac{W_s^* \psi + W_s \psi^*}{2}. \tag{A9}$$

The homogeneous nematic ($f_h^{(n)}$), smectic ($f_h^{(s)}$), and the coupling (f_c) terms determine the equilibrium value of the nematic $[S(\vec{r}) = S_{eq}]$ and smectic $[\eta(\vec{r}) = \eta_{eq}]$ order parameters in a bulk homogeneous sample. The quantities $a_0^{(n)}$, $b^{(n)}$, $c^{(n)}$, T_*, $a_0^{(s)}$, $b^{(s)}$, D, and T_{NA} are positive material constants.

If the smectic and nematic orders are decoupled ($D=0$), the phase behavior of the system is as follows. The quantity T_* determines the supercooling temperature of the isotropic phase, the *I*-*N* transition takes place at $T_{IN} = T_* + \frac{b^{(n)2}}{24a_0^{(n)}c^{(n)}}$, $S_{eq}(T < T_{IN}) = S_0 \frac{3+\sqrt{9-8(T-T_*)/(T_{IN}-T_*)}}{4}$, where $S_0 = S_{eq}(T = T_{IN}) = \frac{b^{(n)}}{4c^{(n)}}$. The Sm*A* phase is reached at $T = T_{NA}$, $\eta_{eq}(T < T_{NA}) = \eta_0 \sqrt{\frac{T_{NA}-T}{T_{NA}}}$, where $\eta_0 = \sqrt{\frac{T_{NA}a_0^{(s)}}{2b^{(s)}}}$.

The elastic term f_e penalizes the departures from the bulk equilibrium ordering. It is expressed in the approximation of equal nematic and smectic elastic constants, where L and C stand for the bare nematic and smectic elastic constants, respectively. The (i) first, (ii) second, and (iii) third terms in the expression for f_e favor (i) homogeneous orientational ordering, (ii) parallel alignment of $\vec{n}$ and the normal $\vec{\nu}_s = \vec{\nabla}\phi/|\vec{\nabla}\phi|$ of a smectic layer, and (iii) the bulk layer distance $d_b = 2\pi/q_0$, respectively. Therefore, in the equilibrium one obtains $\phi = \phi_{eq} = q_0 \vec{r} \cdot \vec{n}$.

The coupling of LC ordering with the CPG surface is described by the nematic ($f_i^{(n)}$) and smectic ($f_i^{(s)}$) interface terms, where W_n and W_s stand for the nematic and smectic anchoring terms and $\vec{\nu}$ is the normal vector of the interface. For nontreated CPG matrices the relation $W_n > 0$ holds favoring perpendicular orientation of LC molecules with respect to $\vec{\nu}$ (the isotropic tangential anchoring condition). In the case of silane-treated samples the relation $W_n < 0$ is fulfilled which favors the orientation of the molecules along $\vec{\nu}$ (the homeotropic anchoring condition). The CPG surface tends to increase the degree of smectic ordering and, thus, the real part of W_s is positive.

The quantities introduced further are the scaled order parameters $\tilde{S} = S/S_0$ and $\tilde{\eta} = \eta/\eta_0$, the reduced temperatures $r_n = \frac{T-T_*}{T_{IN}-T_*}$ and $r_s = \frac{T-T_{NA}}{T_{NA}}$, the dimensionless free-energy density $\tilde{f} = \frac{3f}{2a_0^{(n)}S_0^2}$, and the dimensionless coupling constant $\tilde{D} = \frac{3D\eta_0^2 q_0^2}{2a^{(n)}(T_{IN}-T_*)S_0}$. The coupling with the enclosing interface is neglected and the equality $\phi = \phi_{eq}$ is assumed. Henceforth, the tildes are discarded.

For this parametrization the following expression for the dimensionless free energy of the LC ordering is obtained, for which elastic penalties are absent:

$$f = r_n S^2 - 2S^3 + S^4 + \Omega\left(r_s\eta^2 + \frac{\eta^4}{2}\right) - D\eta^2 S, \tag{A10}$$

where $\Omega = \frac{3\eta_0^2 a_0^{(s)} T_{NA}}{2S_0^2 a_0^{(n)}(T_{IN}-T_*)}$. The equilibrium LC ordering is obtained via minimization of f with respect to S and η. The resulting phase behavior as temperature and coupling strength D are varied is presented in Fig. 6 for a chosen set of parameters. On increasing D two qualitatively changes appear, which are marked by critical values $D = D_c^{(1)}$ and $D = D_c^{(2)}$. Below $D_c^{(1)}$ the *N*-Sm*A* transition is continuous. In the interval $D_c^{(1)} < D < D_c^{(2)}$ the transition becomes discontinuous. Until $D = D_c^{(2)}$ the temperature interval, where the nematic phase is stable, shrinks monotonously. Above $D_c^{(2)}$ the Sm*A* phase is entered directly from the isotropic phase on decreasing T.

[1] *Liquid Crystals in Complex Geometries Formed by Polymer and Porous Networks*, edited by G. P. Crawford and S. Žumer (Oxford University Press, New York, 1996).
[2] T. Bellini, L. Radzihovsky, J. Toner, and N. A. Clark, Science **294**, 1074 (2001).
[3] A. Hourri, T. K. Bose, and J. Thoen, Phys. Rev. E **63**, 051702 (2001).
[4] T. Jin and D. Finotello, Phys. Rev. Lett. **86**, 818 (2001).
[5] G. S. Iannacchione, Fluid Phase Equilib. **222-223**, 177 (2004), and references therein.
[6] G. Cordoyiannis, S. Kralj, G. Nounesis, Z. Kutnjak, and S. Žumer, Phys. Rev. E **75**, 021702 (2007).
[7] G. S. Iannacchione, C. W. Garland, J. T. Mang, and T. P. Rieker, Phys. Rev. E **58**, 5966 (1998).
[8] G. Cordoyiannis, G. Nounesis, V. Bobnar, S. Kralj, and Z. Kutnjak, Phys. Rev. Lett. **94**, 027801 (2005).
[9] G. Cordoyiannis, S. Kralj, G. Nounesis, S. Žumer, and Z. Kutnjak, Phys. Rev. E **73**, 031707 (2006).
[10] T. Bellini, N. A. Clark, C. D. Muzny, L. Wu, C. W. Garland, D. W. Schaefer, and B. J. Olivier, Phys. Rev. Lett. **69**, 788 (1992).
[11] F. M. Aliev and M. N. Breganov, Zh. Eksp. Teor. Fiz. **95**, 122 (1989) [Sov. Phys. JETP **68**, 70 (1989)].
[12] S. Tripathi, C. Rosenblatt, and F. M. Aliev, Phys. Rev. Lett. **72**, 2725 (1994).
[13] M. D. Dadmun and M. Muthukumar, J. Chem. Phys. **98**, 4850 (1993).
[14] Z. Kutnjak, S. Kralj, G. Lahajnar, and S. Žumer, Phys. Rev. E **70**, 051703 (2004).
[15] Z. Kutnjak, S. Kralj, G. Lahajnar, and S. Žumer, Phys. Rev. E **68**, 021705 (2003).
[16] S. Kralj, G. Cordoyiannis, A. Zidansek, G. Lahajnar, H. Amenitsch, S. Žumer, and Z. Kutnjak, J. Chem. Phys. **127**, 154905 (2007).
[17] A. V. Kityk, M. Wolff, K. Knorr, D. Morineau, R. Lefort, and P. Huber, Phys. Rev. Lett. **101**, 187801 (2008).
[18] P. G. de Gennes, Solid State Commun. **10**, 753 (1972).
[19] Y. Imry and S. Ma, Phys. Rev. Lett. **35**, 1399 (1975).
[20] R. L. Leheny, S. Park, R. J. Birgeneau, J. L. Gallani, C. W. Garland, and G. S. Iannacchione, Phys. Rev. E **67**, 011708 (2003).
[21] J. Thoen, H. Marynissen, and W. Van Dael, Phys. Rev. A **26**, 2886 (1982).
[22] G. A. Oweimreen and M. A. Morsy, Thermochim. Acta **346**, 37 (2000).
[23] S. Kralj, A. Zidanšek, G. Lahajnar, I. Muševič, S. Žumer, R. Blinc, and M. M. Pintar, Phys. Rev. E **53**, 3629 (1996).
[24] H. Amenitsch, M. Rappolt, M. Kriechbaum, H. Mio, P. Laggner, and S. Bernstorff, J. Synchrotron Radiat. **5**, 506 (1998).
[25] S. Urban, J. Przedmojski, and J. Czub, Liq. Cryst. **32**, 619 (2005).
[26] P. G. de Gennes and J. Prost, *The Physics of Liquid Crystals* (Oxford University Press, Oxford, England, 1993).
[27] E. Anesta, G. S. Iannacchione, and C. W. Garland, Phys. Rev. E **70**, 041703 (2004).
[28] T. P. Rieker, N. A. Clark, G. S. Smith, D. S. Parmar, E. B. Sirota, and C. R. Safinya, Phys. Rev. Lett. **59**, 2658 (1987).
[29] Y. Ouchi, J. Lee, H. Takezoe, A. Fukuda, K. Kondo, T. Kitamura, and A. Mukoh, Jpn. J. Appl. Phys. **27**, L725 (1988).
[30] S. Kralj and T. J. Sluckin, Phys. Rev. E **50**, 2940 (1994).
[31] D. de las Heras, E. Velasco, and L. Mederos, Phys. Rev. Lett. **94**, 017801 (2005).
[32] M. Kleman and O. Lavrentovich, *Soft Matter Physics* (Springer, New York, 2002).